polymers

MDPI

Article

New Facet in Viscometry of Charged Associating Polymer Systems in Dilute Solutions

Anna Gosteva [1], Alexander S. Gubarev [2], Olga Dommes [1], Olga Okatova [1] and Georges M. Pavlov [1,*]

[1] Institute of Macromolecular Compounds, Russian Academy of Sciences Bolshoi pr. 31, 199004 Saint Petersburg, Russia
[2] Department of Molecular Biophysics and Polymer Physics, Saint Petersburg State University, Universitetskaya nab. 7/9, 199034 Saint Petersburg, Russia
* Correspondence: georges.pavlov@mail.ru

Abstract: The peculiarities of viscosity data treatment for two series of polymer systems exhibiting associative properties: brush-like amphiphilic copolymers—charged alkylated N-methyl-N-vinylacetamide and N-methyl-N-vinylamine copolymer (MVAA-*co*-MVAC$_n$H$_{2n+1}$) and charged chains of sodium polystyrene-4-sulfonate (PSSNa) in large-scale molecular masses (MM) and in extreme-scale of the ionic strength of solutions were considered in this study. The interest in amphiphilic macromolecular systems is explained by the fact that they are considered as micellar-forming structures in aqueous solutions, and these structures are able to carry hydrophobic biologically active compounds. In the case of appearing the hydrophobic interactions, attention was paid to discussing convenient ways to extract the correct value of intrinsic viscosity $[\eta]$ from the combined analysis of Kraemer and Huggins plots, which were considered as twin plots. Systems and situations were demonstrated where intrachain hydrophobic interactions occurred. The obtained data were discussed in terms of $\ln \eta_r$ vs. $c[\eta]$ plots as well as in terms of normalized scaling relationships where η_r was the relative viscosity of the polymer solution. The first plot allowed for the detection and calibration of hydrophobic interactions in polymer chains, while the second plot allowed for the monitoring of the change in the size of charged chains depending on the ionic strength of solutions.

Keywords: associated polymers; intrinsic viscosity; Huggins and Kraemer plots; polymer-polymer interactions

Citation: Gosteva, A.; Gubarev, A.S.; Dommes, O.; Okatova, O.; Pavlov, G.M. New Facet in Viscometry of Charged Associating Polymer Systems in Dilute Solutions. *Polymers* **2023**, *15*, 961. https://doi.org/10.3390/polym15040961

Academic Editors: Artem N. Bezrukov and Asterios (Stergios) Pispas

Received: 20 December 2022
Revised: 7 February 2023
Accepted: 9 February 2023
Published: 15 February 2023

1. Introduction

Amphiphilic polymers have unique properties that are provided by the association of hydrophobic groups and their micro segregation with hydrophilic fragments in aqueous solutions. The association of such polymers in solutions has been studied extensively [1–5]. Amphiphilic polymers are synthesized in the form of various types of block copolymers or molecular brushes when hydrophobic side chains are attached to the hydrophilic main chain of a polymer. Such macromolecules often contain charged groups. In solutions, they exhibit associative properties, which open up possibilities for creating structures that respond to various stimuli and exhibit reversible properties. With an increase in the concentration of solutions, such polymers generate a network structure, where, due to non-covalent interactions, a system of points of non-covalent bonds between different chains (stickers) is formed, which allow for a labile material. Due to the presence of non-covalent interactions (hydrogen bonds, host–guest interactions, electrostatic interactions), amphiphilic polymers acquire new functions that significantly expand their applications.

Such amphiphilic polymers are based on synthetic structures [6–11], as well as on natural polymers [12–15]. They can be used for enzyme immobilization, controlled drug release [16–18], microencapsulation, production of membranes for separation processes, viscosity modifiers for oil production [19–21], and as emulsifiers, dispersants, foaming agents, thickeners, etc. The structures formed in solutions of associating polymers depend

on the concentration of the polymer, the number of attracting groups in the chains, the strength of the physical bonds they form, and the degree of affinity between the polymer and the solvent. In dilute solutions of amphiphilic polymers, intramolecular self-association (i.e., the formation of physical bonds between attracting groups of the same chain) can occur which can lead to a decrease in the size of an individual macromolecule and the formation of loops in it or the formation of a uni-macro-molecular micelle. At high concentrations, the aggregation of several macromolecules into an intermolecular micelle and then to the formation of a physical gel of polymer chains can be observed. Interchain aggregation in a physical network leads to a sharp increase in the viscosity of the solution and the appearance of its high elasticity. These complex dynamic processes in the solutions of associating polymers are extensively studied by suggesting theoretical models of the system of interest [22–27] and rheological methods [28–32].

Rheology studies both the linear viscoelastic behavior of associative polymers, taking into account the density of stickers and the strength of associations with stickers, and the dynamics of associative polymers, determined by the structure of sticker clusters/aggregates and their dissociation [27,33].

In dilute polymer solutions, viscometry serves to determine the characteristics of an isolated macromolecule, following Staudinger [34]. The macromolecules of amphiphilic polymers manifest their peculiar behavior already in dilute solutions, and, as a rule, demonstrate high values of the Huggins parameter [35–38].

The study of the viscous flow of dilute solutions of natural and synthetic polymers has been one of the cornerstones in establishing their macromolecular nature and today is a rather routine but indispensable means to start any polymer investigation. The intrinsic viscosity $[\eta]$ is one of the most important and easily accessible quantities that characterizes the size and conformation of linear polymer molecules. The physical meaning of the $[\eta]$ value of linear polymer molecules is revealed by the Flory–Fox relation: $[\eta] = \Phi\langle h^2\rangle^{3/2}/M$, where $\langle h^2\rangle$ is the mean square distance between the ends of the macromolecular chain, Φ is the hydrodynamic Flory parameter [39].

The intrinsic viscosity was defined by Staudinger as $\lim_{c\to 0}(\eta_{sp}/c) \equiv [\eta]$ [34] and by Kraemer as $\lim_{c\to 0}(\ln\eta_r/c) \equiv [\eta]$ [40], where η_r is relative viscosity, $\eta_{sp} \equiv \eta_r - 1$ is specific viscosity, and c is the concentration of the dissolved substance in g/cm^3. This definition emphasizes that the $[\eta]$ value characterizes a friction of the isolated macromolecule surrounded by solvent molecules. The method of extrapolating the (η_{sp}/c) and $(\ln\eta_r/c)$ values to $c \to 0$ was not indicated by the authors of [34,40]. Various extrapolation plots have been proposed and are still being proposed to determine the intrinsic viscosity of polymers [41–46].

For a long time, and even now, in polymer science the Huggins [47] plot is overwhelmingly used to determine the $[\eta]$ of polymer molecules:

$$\eta_{sp}/c = [\eta]^H + k'[\eta]^2 c + \ldots. \quad (1)$$

Sometimes the Mead–Fuoss plot [46,48] is used. It is also known as the Kraemer plot [40]:

$$\ln\eta_r/c = [\eta]^K + k''[\eta]^2 c + \ldots. \quad (2)$$

Intrinsic viscosity values determined by Equations (1) and (2) are indicated in the text as $[\eta]^H$ and $[\eta]^K$, respectively. At $c \to 0$, these plots should lead to the equivalent estimates of $[\eta]$ value because $\ln\eta_r = \ln(1+\eta_{sp})$ can be expanded into a sign-alternating series in η_{sp} when $\eta_{sp} \le 1$. The equality of the values $[\eta]^H = [\eta]^K$ is an axiomatic condition, i.e., must be performed with a highest level of accuracy. In addition, the mathematical result of this expansion into a mathematical series is: $k'' \equiv k' - 0.5$. As Garcia de la Torre et al. aptly noted [49], the last correlation is just a mathematical consequence that does not correlate with the chemical and physical features of polymer solutions, i.e., the validity of the latter relationship does not depend on either the nature of the solvent or polymer–solvent interactions. Note that the ratio $k'' \equiv k' - 0.5$ is not fulfilled in many cases. Unfortunately, in the literature there are only few works with the simultaneous presence of

the two above-mentioned methods ((1) and (2)). In rare cases, the authors only mention the Kraemer plot, as a rule, without comparing the results obtained. For example, The Polymer Handbook [50] contains extensive tables of the Huggins parameter, but there are no tables for k''.

In this work, the viscometry data were thoroughly analyzed from a methodological and metrological point of view. We demonstrated the obvious need to use the Huggins–Kraemer twin plot in the study of dilute solutions of amphiphilic polymers, as well as neutral linear polymers in thermodynamically poor solvents. First, we demonstrated the evolution of the twin plot for linear polymers as the solvent quality worsening. Then we analyzed the viscometric behavior of the strong linear polyelectrolyte (sodium polystyrene-4-sulfonate (PSSNa)) over wide ranges of both molecular masses (MM) and ionic strengths. In addition, the behavior of brush-like amphiphilic copolymers strong polyelectrolyte (alkylated copolymer of N-methyl-N-vinylacetamide and N-methyl-N-vinylamine (MVAA-co-MVAC$_n$H$_{2n+1}$)) with hydrophobic groups of different lengths in wide ranges of MM and ionic strengths were considered, as well as some data from the literature [51,52]. Finally, the results were discussed in terms of the concept of the normalized Kuhn-Mark-Houwink-Sakurada (KMHS) relationship, which made it possible to compare the results with the full spectrum of possible conformational states of linear macromolecules.

2. Materials and Methods

The synthesis of polymer systems under discussion was described in works [53–56]. The structures of polymers are shown in Scheme 1.

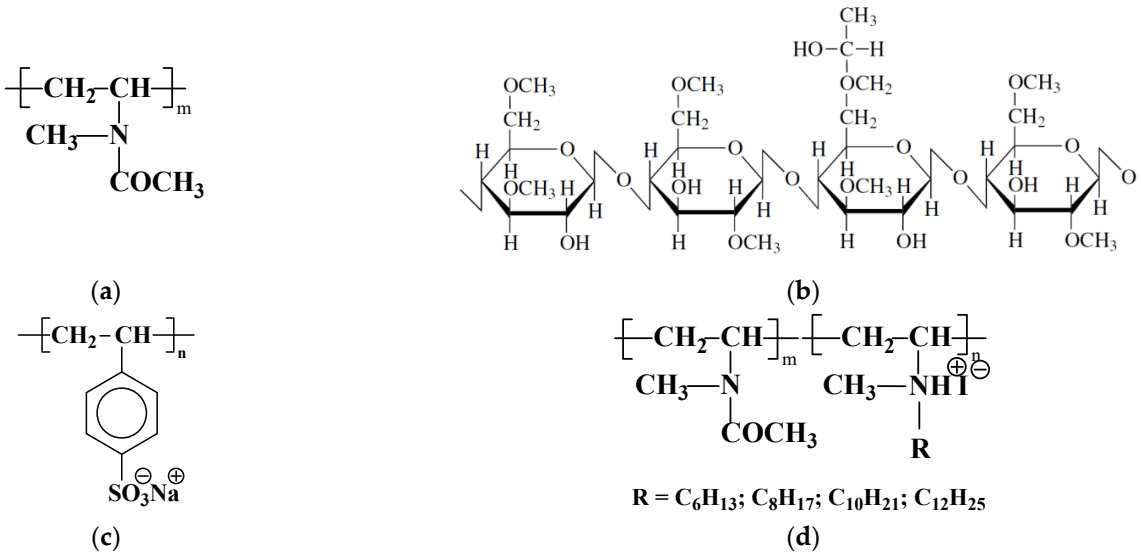

Scheme 1. The structural formula of: (**a**)—poly-N-methyl-N-vinylacetamide homopolymer (PMVA); (**b**)—hydroxypropylmethylcellulose (HPMC); (**c**)—sodium polystyrene-4-sulfonate (PSSNa); and (**d**)—alkylated amphiphilic copolymer of N-methyl-N-vinylacetamide and N-methyl-N-vinylamine (MVAA-*co*-MVAC$_n$H$_{2n+1}$).

The polymers were investigated earlier in water and salt-water solutions by the methods of molecular hydrodynamics: viscometry, sedimentation velocity, and translational diffusion. The results for poly-N-methyl-N-vinylacetamide (PMVA) are described in [57]; for hydroxypropylmethylcellulose (HPMC) in [58]; for PSSNa in [54,59]; for MVAA-*co*-MVAC$_n$H$_{2n+1}$ in [55,60,61]. The copolymer bears charges at the junction of the main and each side chain. The composition of the copolymer is 15 mol.% side chains.

All investigations were carried out at 25 °C. The viscous flow of dilute solutions was investigated in Ostwald capillary viscometer with solvent flow times: 83.5 s (H_2O), 84.1 s (aqueous 0.1 M NaCl), 84.3 s (aqueous 0.2 M NaCl), 120 s (aqueous 4.17 M NaCl). The molecular masses M_{sD} were determined through the Svedberg relationship $M_{sD} = R[s]/[D]$,

where $[s] = s_0\eta_0/(1-\overline{v}\rho_0)$ is the intrinsic sedimentation coefficient, $[D] = D_0\eta_0/T$ is the intrinsic diffusion coefficient, and R is the gas constant. Translational diffusion was studied with a Tsvetkov polarizing diffusometer [48] in a cell [62,63] with optical path 30 mm by classical method of forming a boundary between solvent and solution. The velocity sedimentation was investigated with a Proteomelab XLI (Beckman) ultracentrifuge in a 12-mm two-sector cell at a rotor speed of 40,000 rpm. Sedimentation interference curves were processed with the Sedfit software using general scaling law approach [64,65]. The buoyancy factor $\Delta\rho/\Delta c = (1-\overline{v}\rho_0)$ was measured with a DMA-4000 densitometer (Anton Paar).

3. Results and Discussion

3.1. From Linear Polymers in Thermodynamically Good Solvent through Marginal One and θ-Solvent to Amphiphilic Graft Copolymers

3.1.1. Hydrophylic Flexible Noncharged Nonassociating Poly-N-methyl-N-vinylacetamide (PMVA)

For flexible-chain polymers in thermodynamically good solvents, the k'' parameter is negative and smaller in modulus than the k' parameter. Therefore, the dependence $\ln\eta_r/c$ vs. c changes more slowly with concentration than the dependence η_{sp}/c vs. c. For this reason, as Flory noted, extrapolation $(\ln\eta_r/c)_{c\to0}$ is more preferable than $(\eta_{sp}/c)_{c\to0}$ [66] (page 325). However, Flory's note was not accepted by the polymer community, and the vast majority of information published up to date on the determination of the $[\eta]$ value is derived only from Huggins plots. (See, for example, [50]).

The Huggins and Kraemer classical twin plot for flexible noncharged PMVA in water is shown in Figure 1. In the range of relative viscosities $1.08 < \eta_r < 1.84$ the following results were obtained: from the Huggins plot $[\eta]^H = (107.4 \pm 0.7)$ cm^3/g, $k' = 0.40 \pm 0.02$, $r = 0.9966$ and from the Kraemer plot $[\eta]^K = (107.6 \pm 0.5)$ cm^3/g, $k'' = -(0.12 \pm 0.01)$, $r = 0.9789$ (Sample 4, Table 1). These results testify both the equivalence of the assessment of the main quantity—intrinsic viscosity—by Huggins and Kraemer plots and the validity of the relation $k'' = k' - 0.5$. The data for other PMVA samples [57] are shown in Table 1.

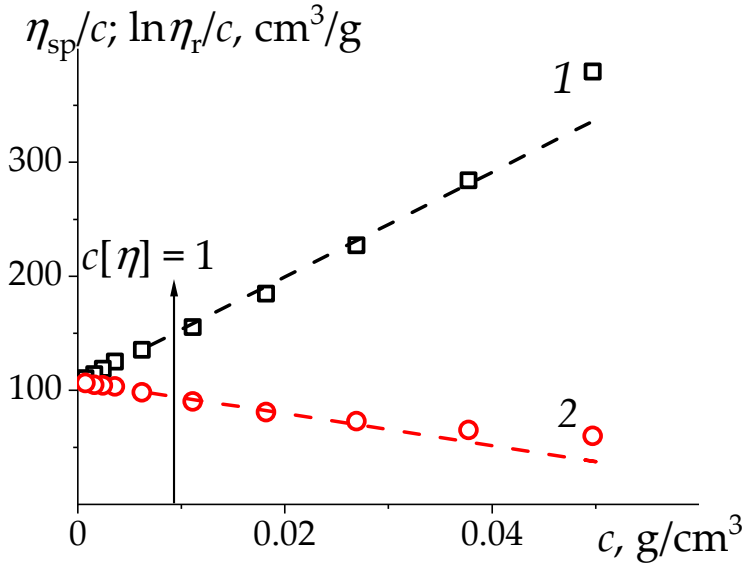

Figure 1. Huggins (1) and Kraemer (2) plots for poly-N-methyl-N-vinylacetamide (PMVA) (sample 4 in Table 1) in H_2O at 25 °C. The values of intrinsic viscosity, Huggins and Kraemer parameters were determined in the interval of relative viscosity: $1.08 < \eta_r < 1.84$ by extrapolation to $c \to 0$. Dashed lines are drawn over the entire range of concentrations and relative viscosities $1.08 < \eta_r < 19.86$.

Table 1. The molecular masses M_{sD} , the values of intrinsic viscosities obtained from Huggins ($[\eta]^H$) and Kraemer ($[\eta]^K$) plots and Huggins (k') and Kraemer (k'') parameters for PMVA in H_2O at 25 °C.

Sample	$M_{sD}10^{-3}$, g/mol	$[\eta]^H$, cm³/g	$[\eta]^K$, cm³/g	k'	$-k''$
1	540	219 ± 4	218 ± 2	0.36 ± 0.04	0.14 ± 0.02
2	440	189 ± 1	188 ± 1	0.35 ± 0.02	0.14 ± 0.02
3	230	113.9 ± 0.2	112.5 ± 0.3	0.23 ± 0.01	0.20 ± 0.01
4	205	107.4 ± 0.7	107.6 ± 0.5	0.40 ± 0.02	0.12 ± 0.01
5	87	55.1 ± 0.1	55.74 ± 0.02	0.49 ± 0.01	0.09 ± 0.01
6	52	40 ± 1	40 ± 1	0.24 ± 0.04	0.22 ± 0.04
7	52	40.4 ± 0.3	40.7 ± 0.1	0.44 ± 0.02	0.11 ± 0.01
8	17	16.1 ± 0.1	16.3 ± 0.1	0.42 ± 0.2	0.08 ± 0.02
9	7.3	10.6 ± 0.5	10.5 ± 0.4	0.44 ± 0.21	0.09 ± 0.15
11	5.2	10.9 ± 0.1	10.9 ± 0.1	0.05 ± 0.03	0.38 ± 0.04
12	6.7	8.5 ± 0.1	8.6 ± 0.1	0.41 ± 0.08	0.13 ± 0.05

The average deviation between the $[\eta]^H$ and $[\eta]^K$ values is 0.7%, and $(k' - k'') = 0.50 \pm 0.015$ over the entire Table 1 data array. It should be noted that for flexible-chain polymers in thermodynamically good solvents, relations (1) and (2) usually lead to virtually the same value $[\eta]$, and the ratio $k'' = k' - 0.5$ is also practically fulfilled. This kind of accuracy is common for the viscosity measurements of flexible macromolecules.

This led to the fact that in the most studies, the use of the Kraemer plot was considered an unnecessary waste of time and the process of determining $[\eta]$ value has been optimized as much as possible, i.e., only the Huggins plot was used.

3.1.2. Peculiarities of Viscosity Behavior of Associating Systems

As the thermodynamic quality of the solvent worsens, the absolute value of the parameter k'' decreases to zero, and then becomes positive and continues to increase. The parameter k' continuously increases in this case.

The slope of $\ln \eta_r / c$ vs. c (Equation (2)) is the quantity $(k''[\eta]^2)$. When $k'' \approx 0$, this dependence in the region of dilute solutions looks like some "fluctuation" of $\ln \eta_r / c$ values depending on the concentration. Apparently, it is this range of k'' values that induces doubt among experimenters about the reliability of intrinsic viscosity determining from Kraemer plot. Indeed, in this case, this dependence may have a small or extremely small linear correlation coefficient. However, *this does not mean that in this case the main sought value* $[\eta]$ *becomes less certain when using the Kraemer plot compared to the Huggins plot*. When $k'' \approx 0$ the absolute error in determining k'' is greater than its value. But nevertheless, the absolute error in determining $[\eta]^K$ is practically the same as that of $[\eta]^H$ for the same data set. The $k'' \approx 0$ is typical for thermodynamically poor or marginal solvents, i.e., solvents approaching the θ-solvent in terms of their thermodynamic quality.

An example of such a rare system is shown in Figure 2 with a treatment of our viscometric data for a water-soluble hydroxypropylmethylcellulose (HPMC) sample with the degrees of substitution of 1.90 for methoxy and 0.26 for hydroxypropyl groups and with a MM of 207,000 g/mol. MM was calculated from the KMHS ratio established for HPMC samples studied in water [58].

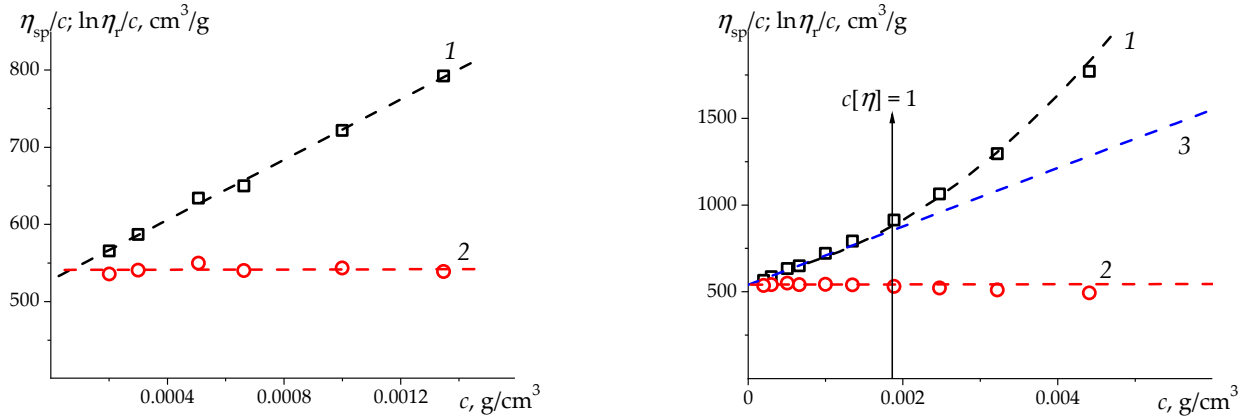

(**a**) (**b**)

Figure 2. The Huggins (1) and Kraemer (2) plots for a sample of hydroxypropylmethylcellulose (HPMC) (M_{sD} = 207,000 g/mol) in H_2O at 25 °C [58]: (**a**)—in the range of relative viscosities $1.11 < \eta_r < 2.07$, where extrapolation to $c \to 0$ was carried out and the values of intrinsic viscosity and Huggins and Kraemer parameters were determined $[\eta]^H = (528 \pm 4)$ cm^3/g, $k' = 0.70 \pm 0.03$, $r = 0.9984$;$[\eta]^K = (541 \pm 4)$ cm^3/g, $k'' = +(0.002 \pm 0.02)$, $r = 0.0637$; $0.11 < c[\eta] < 0.73$); (**b**)—in the entire range of concentrations (Line 3 is drawn as a tangent to the 2-nd degree polynomial fit in the initial range of values $\eta_r < 1.4$ which corresponds to following values: $[\eta]^H = 540$ cm^3/g, $k' = 0.35$. Overall parabola (1) demonstrates the curvature of dependence of η_{sp}/c in contrast with one of $\ln \eta_r/c$ in the entire interval $1.11 < \eta_r < 8.8$).

The difference between the estimates of $[\eta]$ from the two plots (Figure 2a) is $[\eta]^K/[\eta]^H \approx 2.5\%$, which is usually not considered significant. Obviously, in this case, there is a good agreement between the $[\eta]^H$ and $[\eta]^K$ values. However, this is 3.5 times greater than the deviation observed for the flexible chain PMVA (Table 1). It is noteworthy that the coefficient of linear correlation of the Huggins plot is $r = 0.9984$, whereas this coefficient for the Kraemer plot is $r = 0.0637$, which means that the slope of the Kraemer plot is practically zero. At the same time, the absolute errors of the $[\eta]$ value for the two plots practically coincide $\Delta[\eta]^K = \Delta[\eta]^H = 4$ cm^3/g.

The value of the Kraemer parameter $k'' \approx 0$ indicates that water is not a thermodynamically good solvent for hydroxypropylmethylcellulose. It can be expected that as the concentration of solutions increases, the dependences will clearly show the hydrophobicity of this polymer. Indeed, Figure 2b shows a noticeable difference in the behavior of the Kraemer and Huggins dependences in the interval $c[\eta] > 1$. The dependence of η_{sp}/c on c increases sharply and can be approximated by a parabola, while the dependence of $\ln \eta_r/c$ changes slightly. In this regard, we have carried out a correction of the η_{sp}/c in the low concentrations. For this, we formed a data system consisting of experimental values η_{sp}/c at the $\eta_r < 1.4$ and add to them a point ($c = 0$, $\eta_{sp}/c = [\eta]^K$), taking into account an axiom $[\eta]^H \equiv [\eta]^K$. We processed this data with a second degree polynomial function and draw the tangent to it at $c = 0$. The tangent equation is $\eta_{sp}/c = 540 + 10.25c$, i.e., $[\eta]^H_{corr} = 540$, $k'_{corr} = 0.35$. Thus, a slight increase in $[\eta]^H$ by 2.3% leads to a twofold decrease in the Huggins parameter. In a similar way, we processed the data of η_{sp}/c in the region of extremely dilute solutions for the amphiphilic polymer systems.

Note that Garcia de la Torre et al. had already developed the program for linear least-square fits with a common intercept [67] for systems with a negative value of the Kraemer parameter. It would be useful to adapt the program for joint processing of the Huggins and Kraemer plots for the associating polymer systems with a positive value of the Kraemer parameter, as suggested above and below.

With a further decrease in the polymer-solvent affinity and an increase in the role of polymer-polymer interactions compared to polymer-solvent interactions, the parameter k'' changes sign to positive. The relation $k'' = k' - 0.5$ is no more valid. However, in all cases, the k'' parameter is less in absolute value than the parameter k', therefore, the dependence $\ln \eta_r / c$ will remain linear in a larger concentration range compared to the dependence η_{sp}/c.

This situation is illustrated by an charged brush-like alkylated amphiphilic copolymer of N-methyl-N-vinylacetamide and N-methyl-N-vinylamine, which combines a hydrophilic charged base and hydrophobic $C_{12}H_{25}$ side groups (MVAA-*co*-MVAC$_{12}$H$_{25}$) [55,61] (Figure 3) and linear homopolymer PSSNa, which exhibits hydrophobic interactions in θ-solvent [54,59,68] (Figure 4).

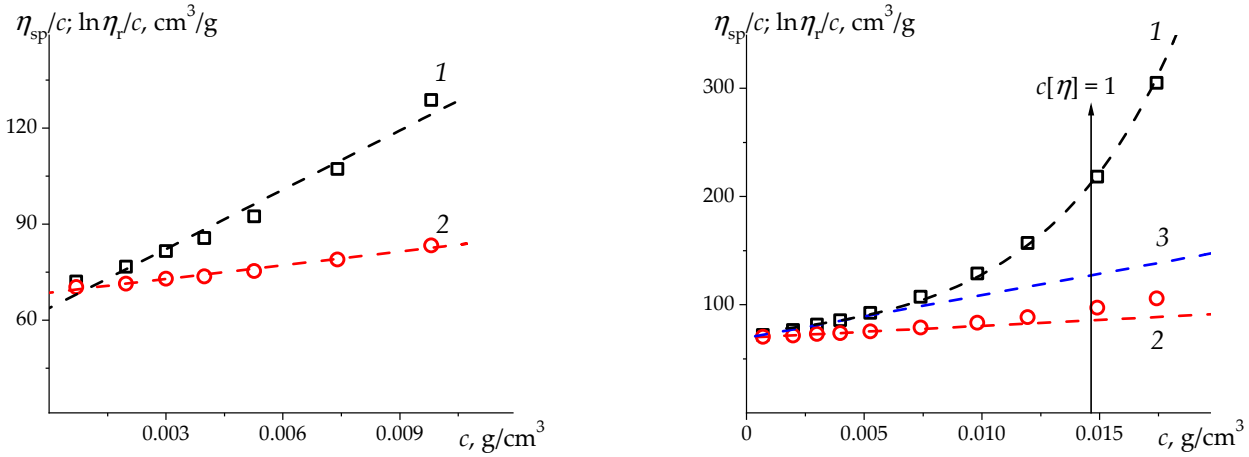

Figure 3. The Huggins (1) and Kraemer (2) plots for alkylated copolymer of N-methyl-N-vinylacetamide and N-methyl-N-vinylamine (MVAA-*co*-MVAC$_{12}$H$_{25}$) [55,61] (Sample 4 in Table 4) in aqueous 0.1 M NaCl solution at 25 °C: (**a**)—in the range of relative viscosities $1.05 < \eta_r < 2.25$ ($[\eta]^H = (64 \pm 3)$ cm^3/g, $k' = 1.5 \pm 0.2$, $r = 0.9863$; $[\eta]^K = (68.6 \pm 0.5)$ cm^3/g, $k'' = +(0.30 \pm 0.02)$, $r = 0.9917$); and (**b**)—in the entire range of concentrations $1.05 < \eta_r < 6.35$ (Line 3 is drawn as a tangent to the 2-nd degree polynomial fit in the initial range of values $\eta_r < 1.5$, its values: $[\eta]^H_{corr} = 68.9$ cm^3/g, $k'_{corr} = 0.88$. Overall parabola (1) demonstrates the curvature of dependence of η_{sp}/c in contrast with one of $\ln \eta_r/c$ in the entire interval $1.05 < \eta_r < 6.35$).

The results obtained in this way for all investigated PSSNa fractions in aqueous 4.17 M NaCl, are presented in Table 2. The $[\eta]^H$ values obtained by direct linear extrapolation of η_{sp}/c (let's indicate it $[\eta]^H_{brutto}$) in the entire dataset are lower than $[\eta]^K$ values, and the error in determining $[\eta]^H$ is noticeably greater than that for $[\eta]^K$. After the $[\eta]$ values are converged to a single value corresponding to $[\eta]^K$, the corrected values of the Huggins parameter are reduced by 2–6 times compared to the k'_{brutto} values obtained by simple linear treatment (Figure 3a, line 1, Figure 4a, line 1). A consistent estimate of $[\eta]$ will lead to a change in both parameters of the Kuhn-Mark-Houwink-Sakurada ratio and, accordingly, to a refinement of the conformational status of PSSNa macromolecules in aqueous 4.17 M NaCl compared to estimates based on $[\eta]^H$ [54].

The most important postulate when using the Huggins and Kraemer plots is the statement that $\lim\limits_{c\to 0}(\eta_{sp}/c) \equiv \lim\limits_{c\to 0}(\ln \eta_r/c)$, i.e., the dependencies must converge at one point on the y-axis at $c = 0$. However, for many polymer systems the intercept on the y-axis at $c = 0$ on Huggins plot is less than that on Kraemer one. That is, from the Huggins plot, we get a somewhat underestimated value of the intrinsic viscosity, while the brutto values of the Huggins parameter will be quite large, the larger is the value of k''. In the considered Figures 2–4, the initial values of $[\eta]^H_{brutto}$ are less than $[\eta]^H_{brutto}$ by 2.3, 7.1 and

34%, respectively. When $[\eta]^{H}$ is corrected to $[\eta]^{K}$, the Huggins parameter decreases by factors of 2.0, 1.7, and 2.8, respectively, compared to its brutto values. The correlation between k' and k'' over the entire range of their values requires more detailed study for a wide set of polymer systems.

Table 2. The molecular masses M_{sD} , the values of intrinsic viscosities, obtained from Huggins ($[\eta]^{H}_{brutto}$) and Kraemer ($[\eta]^{K}$) plots and Kraemer (k'') and Huggins (k'_{brutto}, k'_{corr}) parameters for PSSNa in aqueous 4.17 M NaCl solutions at 25 °C.

Sample	$M_{sD}10^{-3}$, g/mol	$[\eta]^{H}_{brutto}$, cm³/g	$[\eta]^{K}$, cm³/g	$[\eta]^{K}/[\eta]^{H}_{brutto}$	k''	k'_{brutto}	k'_{corr}
PSSNa-2	847	11.9 ± 0.6	14.5 ± 0.1	1.22	1.8 ± 0.1	5.5 ± 0.9	2.1 ± 0.2
PSSNa-3	607	14.4 ± 1.0	17.2 ± 0.2	1.19	1.1 ± 0.1	3.9 ± 0.9	1.4 ± 0.2
PSSNa-4	605	11.0 ± 0.6	14.3 ± 0.1	1.30	1.4 ± 0.1	5.7 ± 0.9	1.6 ± 0.1
PSSNa-5	448	9.5 ± 0.7	12.7 ± 0.1	1.34	1.6 ± 0.1	7 ± 2	1.8 ± 0.1
PSSNa-6	375	9.6 ± 0.9	12.3 ± 0.2	1.27	1.4 ± 0.1	6 ± 2	1.6 ± 0.2
PSSNa-7	124	3.6 ± 0.5	5.9 ± 0.1	1.64	2.1 ± 0.2	14 ± 5	3.2 ± 0.6
PSSNa-8	84	2.9 ± 0.6	6.0 ± 0.2	2.03	2.1 ± 0.1	23 ± 15	1.7 ± 0.3
PSSNa-9	53	3.0 ± 0.4	5.3 ± 0.1	1.77	1.8 ± 0.1	15 ± 6	1.8 ± 0.2

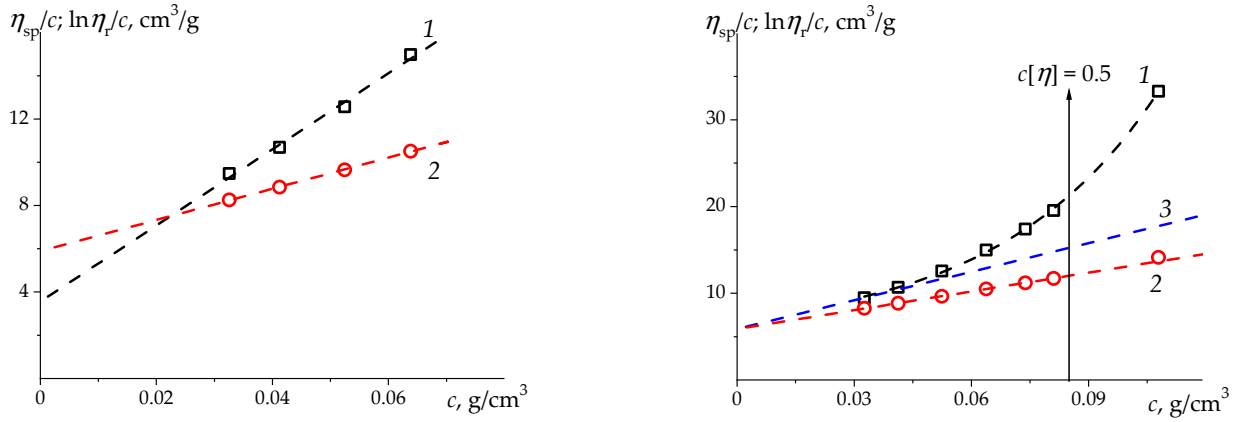

Figure 4. The Huggins (1) and Kraemer (2) plots for sodium polystyrene-4-sulfonate (PSSNa) (sample PSSNa-7 in Table 2) in aqueous 4.17 M NaCl (θ-solvent at 25 °C) [54,59] with different data approximation: (**a**)—linear fits (lines 1 and 2) in the range of relative viscosities $1.45 < \eta_r < 1.96$ ($[\eta]^{H} = (3.6 \pm 0.5)$ cm³/g, $k' = 14 \pm 5$, $r = 0.9960$ (1); $[\eta]^{K} = (5.89 \pm 0.05)$ cm³/g, $k'' = +(2.08 \pm 0.07)$, $r = 0.9998$ (2)); and (**b**)—overall parabola η_{sp}/c (1) in the full measured range $1.45 < \eta_r < 4.6$, Kraemer linear fit (line 2), and tangent (line 3) to the 2-nd degree polynomial fit in the range $\eta_r < 1.45$ (which (3) leads to the values $[\eta]^{H}_{corr} = 5.89$ cm³/g, $k'_{corr} = 3.2$). Overall parabola η_{sp}/c (1) is drawn for clarity in order to emphasize the curvature of the dependence in the interval $1.45 < \eta_r < 4.6$).

3.2. Viscometric Data at Different Ionic Strengths of Solutions

3.2.1. Sodium poly(Styrene-4-Sulfonate)

Equation (2) can be represented as the dependence of $\ln \eta_r$ on the Debye parameter ($c[\eta]$):

$$\ln \eta_r = c[\eta] + k''(c[\eta])^2 + \ldots. \quad (3)$$

The Debye parameter $c[\eta]$ characterizes the dilution degree of the solution.

This is a well-known plot in rheology which allows one to compare viscosity data for polymers with various molecular masses and chemical structures, and in different solvents.

Over a wide concentration range the dependence $\ln \eta_r$ on $c[\eta]$ is described by a second-degree polynomial:

$$\ln \eta_r = A + B_1(c[\eta]) + B_2(c[\eta])^2 + \ldots. \quad (4)$$

According to the Kraemer definition of $[\eta]$, its initial slope B_1 (at $c \to 0$) is equal to 1. The second derivative B_2, determined in the region of dilute solutions, is the Kraemer parameter k''. Its sign determines the trend of the dependence. Thus, at $c \to 0$ with $A \approx 0$, $B_1 \approx 1$, and $B_2 \approx k''$ the relationship (4) is transformed into (3).

The plot $\ln \eta_r = f(c[\eta])$ for PSSNa in aqueous 4.17 M NaCl (a), aqueous 0.2 M NaCl (b), and in salt-free water (e) solutions at 25 °C as well as the data for two polystyrene (PS) samples with MM 146,000 and 600,000 g/mol in toluene at 30 °C (points c and d) [52] are shown in Figure 5.

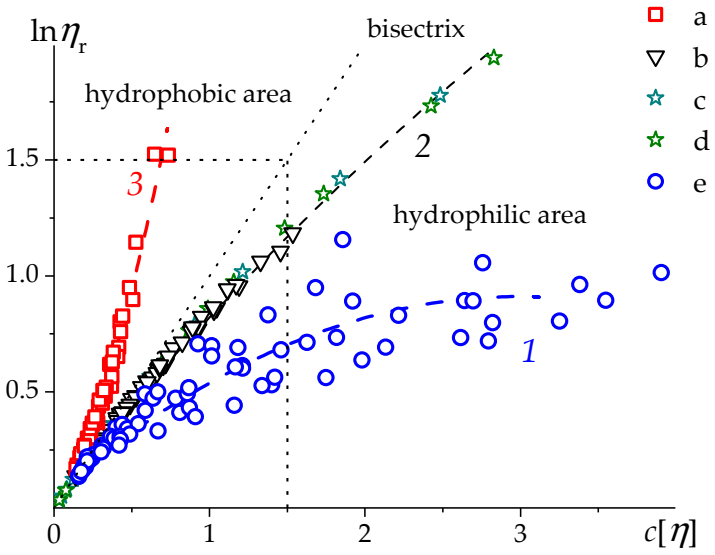

Figure 5. The dependence of natural logarithm of relative viscosity $\ln \eta_r$ vs. $c[\eta]$ resolved for PSSNa in aqueous solutions of different ionic strength [54,59] (a—4.17 M NaCl, $B_2 = (2.9 \pm 0.6)$; b—0.2 M NaCl, $B_2 = -(0.043 \pm 0.002)$, and e—H_2O, $B_2 = -(1.4 \pm 0.4)$) and polystyrene (PS) in toluene, $B_2 = -(0.12 \pm 0.01)$ [52] (c and d—samples with $M = 146{,}000$ and 600,000 g/mol, correspondingly). Dashed line represents the bisectrix (i.e., line $\ln \eta_r = c[\eta]$) of current coordinates, 1—is extrapolation of PSSNa data in H_2O (e), 2—PSSNa in aqueous 0.2 M NaCl (b), PS in toluene (c and d), and 3—PSSNa in aqueous 4.17 M NaCl (a).

The points for PSSNa in aqueous 0.2 M NaCl solutions (b in Figure 5) for all fractions fit into virtualy single convex dependence, i.e., characterized by a negative second derivative ($B_2 < 0$), which corresponds to a negative value of the Kraemer parameter (Table 3). Note that the data on the toluene-soluble fractions of PS (c, d in Figure 5) [52], fit well into a single dependence with PSSNa in aqueous 0.2 M NaCl. This means that these macromolecules are in virtually identical thermodynamic conditions. The PSSNa data in aqueous 4.17 M NaCl solution (a θ-solvent at 25 °C [54,69], form a single concave curve, which corresponds to positive values of both B_2 and k''. The space defined by coordinates $\ln \eta_r = f(c[\eta])$ can be divided into two parts by a straight line $\ln \eta_r = c[\eta]$ (bisecrix) corresponding to the condition $B_2 = 0$ ($k'' = 0$). To the right is an area of hydrophilic systems and/or systems that are in thermodynamically good conditions; to the left is an area of hydrophobic and/or systems near θ-conditions. Note that, both in aqueous 0.2 M and 4.17 M NaCl solutions, the system of PSSNa fractions manifests itself as a molecular homologues system. In salt-free solutions (points e in Figure 5), the fractions of charged PSSNa macromolecules do not form a single dependence. This situation will be discussed below.

Table 3. The molecular masses M_{sD} , the values of intrinsic viscosities, obtained from Huggins ($[\eta]^H$) and Kraemer ($[\eta]^K$) plots, and Huggins (k') and Kraemer (k'') parameters for PSSNa in aqueous 0.2 M NaCl at 25 °C.

Sample	$M_{sD}10^{-3}$, g/mol	$[\eta]^H$, cm³/g	$[\eta]^K$, cm³/g	k'	$-k''$
PSSNa-1	1500	372 ± 3	368 ± 3	0.28 ± 0.02	0.17 ± 0.01
PSSNa-2	847	174 ± 1	173.4 ± 0.6	0.35 ± 0.01	0.14 ± 0.01
PSSNa-3	607	170 ± 3	168 ± 2	0.32 ± 0.04	0.16 ± 0.02
PSSNa-4	605	117 ± 1	117 ± 1	0.40 ± 0.03	0.12 ± 0.02
PSSNa-5	448	117 ± 1	115.7 ± 0.4	0.29 ± 0.02	0.17 ± 0.01
PSSNa-6	375	109 ± 1	108 ± 1	0.29 ± 0.02	0.16 ± 0.01
PSSNa-7	124	43.5 ± 0.6	43.3 ± 0.4	0.33 ± 0.03	0.16 ± 0.01
PSSNa-8	84	29.8 ± 0.4	29.2 ± 0.1	0.31 ± 0.02	0.15 ± 0.01
PSSNa-9	53	22.0 ± 0.2	21.8 ± 0.2	0.32 ± 0.02	0.15 ± 0.01
PSSNa-10	51	20.0 ± 0.1	20.0 ± 0.1	0.36 ± 0.01	0.14 ± 0.01

In contrast with data in Table 2 (PSSNa in 4.17 M NaCl) the average deviation between the $[\eta]^H$ and $[\eta]^K$ values is 0.8%, and $(k' - k'') = 0.48 \pm 0.01$ over the entire Table 3 data array in 0.2 M NaCl. This is similar to statistic of Table 1 for noncharged PMVA in H_2O.

Note that despite the demonstration of associative properties in 4.17 M NaCl, PSSNa macromolecules behave both in 0.2 M and 4.17 M NaCl as a homologous series (Figure 5).

3.2.2. Alkylated Random Copolymers of N-Methyl-N-Vinylacetamide and N-methyl-N-vinylamine (MVAA-*co*-MVAC$_n$H$_{2n+1}$)

For brush-like amphiphilic copolymers with hydrophobic side chains and hydrophilic backbone an important structural parameter is the ratio of the average distance between two neighboring alkyl side chains (l_{phil}) to contour length of their side chain (l_{phob}). This parameter (l_{phil}/l_{phob}) characterizes the ratio between hydrophilic and hydrophobic parts in a copolymer molecule. The MVAA-*co*-MVAC$_{12}$H$_{25}$ random copolymer has such a composition of the side aliphatic groups (15 mol.%) when the average distance between adjacent side groups is almost equal to the contour length of the C$_{12}$H$_{25}$ side group ($l_{phil} \approx l_{phob}$). These copolymers, being strong polyelectrolytes, are readily soluble in salt-free water, and being flexible-chain in nature, they strongly react to changes in the ionic strength of the solution.

As follows from the viscometric plots, the primary polyelectrolyte effects are suppressed in aqueous 0.1 M NaCl solutions. The viscometric data for MVAA-*co*-MVAC$_n$H$_{2n+1}$ are given in Figure 6 and Table 4. The data in Figure 6 are presented in $\ln \eta_r$ vs. $c[\eta]$ coordinates with the division of space into two regions: hydrophobic and hydrophilic.

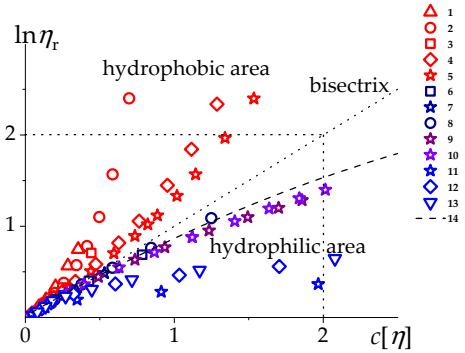

Figure 6. The dependence of the $\ln \eta_r$ on the degree of dilution $c[\eta]$ for MVAA-*co*-MVAC$_{12}$H$_{25}$ with different molecular masses in aqueous 0.1 M NaCl (1–5), DMFA + 0.1 M LiCl (6–8), in H_2O (11–13), MVAA-*co*-MVAC$_6$H$_{13}$ (9) and MVAA-*co*-MVAC$_8$H$_{17}$ (10) in aqueous 0.1 M NaCl solution and PMVA in H_2O (14). The dashed line $\ln \eta_r = c[\eta]$ separates two regions: the region of polymers with hydrophobic interactions and the region of polymers with hydrophilic interactions.

Table 4. The molecular masses M_{sD}, the values of intrinsic viscosities, obtained from Huggins ($[\eta]^H$) and Kraemer ($[\eta]^K$) plots and Huggins (k') and Kraemer (k'') parameters, for MVAA-*co*-$MVAC_{12}H_{25}$ in aqueous 0.1 M NaCl (Samples 1–5) and DMFA + 0.1 M LiCl (Samples 6–8); MVAA-*co*-$MVAC_6H_{13}$ (Sample 9) and MVAA-*co*-$MVAC_8H_{17}$ (Sample 10) in aqueous 0.1 M NaCl.

Sample	Solvent	$M_{sD}10^{-3}$, g/mol	$[\eta]^H$, cm³/g	k'	$[\eta]^K$, cm³/g	k''	B_2
1	0.1 M NaCl	77	12 ± 2	16 ± 5	18,5 ± 0,9	3.2 ± 0,5	3.7 ± 0.2
2		151	36 ± 3	4 ± 1	41 ± 2	1.5 ± 0.3	1.7 ± 0.2
3		151	42 ± 5	6 ± 2	54 ± 2	1.3 ± 0,2	1.39 ± 0.08
4		156	64 ± 3	1.52 ± 0.2	68.6 ± 0.5	0.30 ± 0.02	0.31 ± 0.02
5		149	64 ± 2	1.7 ± 0.2	72 ± 2	0.30 ± 0.07	0.25 ± 0.05
6	DMFA + 0.1 M LiCl	148	65.3 ± 0.6	0.32 ± 0.03	65.1 ± 0.5	–0.16 ± 0.01	−0.15 ± 0.02
7		-	64.8 ± 0.2	0.32 ± 0.01	64.6 ± 0.2	–0.165 ± 0.008	−0.165 ± 0.008
8		55	37.9 ± 0.4	0.43 ± 0.03	38.2 ± 0.2	–0.12 ± 0.01	−0.108 ± 0.008
9	0.1 M NaCl	98	102.9 ± 0.8	0.26 ± 0.02	101.8 ± 0.3	–0.189 ± 0.007	−0.196 ± 0.005
10		97	104.3 ± 0.5	0.23 ± 0.01	103.2 ± 0.2	–0.205 ± 0.005	−0.208 ± 0.004

Despite the fact that the samples have the same chemical composition, the viscometric results do not fit into a single curve but represent a set of curves with different values of the positive second derivative B_2. Thus, the samples can be differentiated by the level of hydrophobicity: the more B_2, the more the sample is hydrophobic. As a result, the homology of the studied series is violated, which is associated evidently with their irregular, random distribution of $C_{12}H_{25}$ side groups along the chain.

In DMF + 0.1 M LiCl solutions of MVAA-*co*-$MVAC_{12}H_{25}$ the hydrophobicity effect "turns off" and the viscometric results (points 6–8, Figure 6) are in good agreement with the data obtained for the parent uncharged homopolymer PMVA (dashed curve, Figure 6). In organic solvents, where hydrophobic interactions are absent, these copolymers behave as polymer homologues.

Note that samples with short aliphatic groups C_6H_{13} and C_8H_{17} (points 9 and 10, Figure 6) do not exhibit hydrophobic behavior in 0.1 M NaCl solutions at all, being located near the data corresponding to the homopolymer. For these copolymers (with the composition mol. 15%), the contour length of the side radicals is much less than the average distance between them along the main chain. In this case, the total share of hydrophobicity of the macromolecule is less than the share of hydrophilicity.

For the studied copolymers the ratio l_{phil}/l_{phob} changes within the limits: $1.03 < l_{phil}/l_{phob} < 1.90$. When $l_{phil}/l_{phob} \approx 1$, intramolecular hydrophobic interactions occur in the copolymer; when $l_{phil}/l_{phob} > 1.5$ they are not observed. The latter is shown in Figure 6 for MVAA-*co*-$MVAC_6H_{13}$ (points 9) and MVAA-*co*-$MVAC_8H_{17}$ (points 10) in aqueous 0.1 M NaCl solutions.

3.2.3. The Behaviour of Polymers in Salt-Free Solutions

The two studied systems PSSNa and MVAA-*co*-$MVAC_{12}H_{25}$ are strong polyelectrolytes. The $[\eta]$ value was determined from initial slope of the dependence of $\ln \eta_r$ on c according to the Kraemer definition $\lim_{c\to 0}(\ln \eta_r/c) \equiv [\eta]$ [40,56,70].

The results on PSSNa are presented at Figures 7 and 8, and in Table 5. For comparison, the data from the unique viscometric study of PSSNa in H_2O [51] were added to Figure 8.

In salt-free solutions of highly charged linear chains, electrostatic interactions are dominant.

Irregular re-condensation of counterions onto a charged chain leads to a statistical distribution of charges along the chain and loss of homology of such polymer series in salt-free solutions.

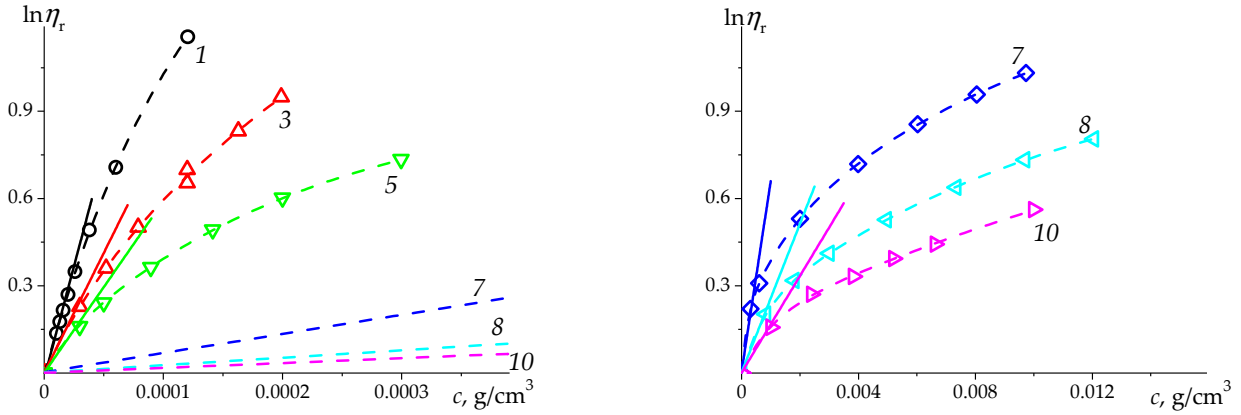

(**a**) (**b**)

Figure 7. The natural logarithm of relative viscosity $\ln \eta_r$ vs. concentration c for PSSNa data in H_2O at 25 °C. The dashed curves are the 2-nd degree polynomial fit of the presented data sets, the solid lines correspond to the initial slope of the dependences representing the intrinsic viscosity value, as $[\eta] = d(\ln \eta_r)/dc$ at $c = 0$. The numbers next to the lines correspond to the sample numbering in the Table 5. The lines 7, 8 and 10 on the (**a**) represent the slopes from the (**b**).

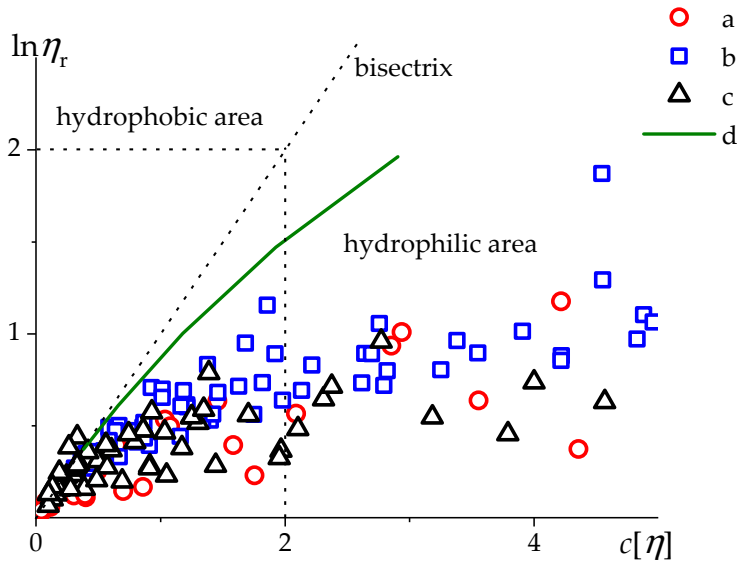

Figure 8. The dependence of natural logarithm of relative viscosity $\ln \eta_r$ on dilution degree $c[\eta]$ resolved in H_2O solution for PSSNa (a—[51], b—[54]), MVAA-*co*-MVAC$_{12}$H$_{25}$ (c—[55], and PMVA [57] (d, sample 4 in Table 1). Dashed line is the bisectrix of current coordinates (i.e., line $\ln \eta_r = c[\eta]$).

One can see that the points for all charged polymers (a, b, c in Figure 8) lie below the line d for a neutral water-soluble homopolymer PMVA. It is explained by the fact that with an increase in the concentration of the polyelectrolyte in pure water, the ionic strength of the solution increases due to an increase in the number of counterions in the solution, and the coils shrink. As $c[\eta]$ increases, the interaction of hydrophobic C_{12} side groups slightly appears. The dependence at Figure 8 demonstrates a weak manifestation of the hydrophobicity of MVAA-*co*-MVAC$_{12}$H$_{25}$ in comparison with the PSSNa. The MVAA-*co*-MVAC$_{12}$H$_{25}$ data (points c in Figure 8) lie a little bit lower in the region $c[\eta] > 2$ than that for PSSNa (points a, b in Figure 8).

At very high values of polymer charge density and low ionic strength, the level of hydrophobicity practically does not affect the size of polyelectrolyte chains.

Table 5. The molecular masses M_{sD}, the values of intrinsic viscosities $[\eta]$ and parameters B_2 (Equation 4) for PSSNa in H_2O at 25 °C.

Sample	$M_{sD}10^{-3}$, g/mol	$[\eta]$, cm^3/g	$-B_2$
PSSNa-1	1500	15,400 ± 300	0.21 ± 0.03
PSSNa-2	847	8900 ± 60	0.39 ± 0.01
PSSNa-3	607	8200 ± 90	0.36 ± 0.02
PSSNa-4	605	5100 ± 30	0.57 ± 0.02
PSSNa-5	448	5900 ± 50	0.59 ± 0.02
PSSNa-6	375	4800 ± 200	0.47 ± 0.08
PSSNa-7	124	660 ± 40	0.46 ± 0.04
PSSNa-8	84	260 ± 10	0.59 ± 0.07
PSSNa-9	53	135 ± 7	0.58 ± 0.08
PSSNa-10	51	167 ± 6	0.76 ± 0.06

3.3. Normalized Scaling Relationships: Comparison of Viscometric Data

Intrinsic viscosity is the most sensitive characteristic to the size, shape, and their change for linear macromolecules in solutions. This is why the Kuhn-Mark-Houwink-Sakurada relationship ($[\eta] = K_\eta M^{b_\eta}$) is so popular in polymer science. To date, an extensive library of these relationships for polymers of various structures and in various solvents has been formed and is being replenished [71]. If we put all these data on the lg$[\eta]$ vs. lg$M$ plot, we get a rather chaotic filling of this two-dimensional space. However, it turned out that this "pointillist picture" is transformed into a fairly clear ordered structure of the viscometric spectrum of linear macromolecules of different nature and structure, unfolded in size, if we take into account on this plot the mass of a linear chain length unit (M_L), which characterizes the linear density of the macromolecule [72–74]. This transformation follows from the fundamental Flory–Fox relation that $[\eta]M_L \sim < h^2 >^{3/2}/L \sim V/L$, where V is the volume occupied by the macromolecule in solution. Consequently, the value $[\eta]M_L$ characterizes the volume occupied by the chain segment corresponding to the unit contour length of the macromolecule (which is conveniently chosen as a repeating link). This value will be the greater, the greater is the equilibrium rigidity of the macromolecule and the better is the thermodynamic quality of the solvent. Thus, by transforming the standard plot lg$[\eta] = f(\lg M)$ used to establish the classical KMHS relation, we obtained the plot $(\lg([\eta]M_L) = f(\lg(M/M_L))$, which represents a sweep by their sizes of the entire spectrum of linear macromolecules so far studied. Linear macromolecules were divided into the following classes: extra-rigid, rigid, flexible in thermodynamically good solvents, flexible under θ-conditions, and globular. This plot is the result of an analysis of a large number of data in the literature and covers the area of macromolecules contour lengths changing by three orders of magnitude and the area of equilibrium rigidities of linear chains changing by approximately 500 times. Thus, by applying the experimental data to the obtained template/sweep, one can judge whether the studied polymer belongs to one or another class of linear polymers and get an idea of the length of the statistical segment or the persistent length of the chain. Let us analyze the results discussed in this paper in the coordinates $\lg([\eta]M_L)$ vs. $\lg(M/M_L)$ (Figure 9).

The joint manifestation of electrostatic long-range effects and short-range interaction leads to the maximum sizes of charged chains in salt-free solutions of both PSSNa chains and MVAA-*co*-$MVAC_{12}H_{25}$ chains (points 2 and 5). In the salt-free solutions, the hydrophobicity of the chains does not manifest in any way. Despite the different composition (PSSNa—100 mol.% and MVAA-*co*-$MVAC_nH_{2n+1}$—15 mol.%), these chains are strong polyelectrolytes [61,75]. As the ionic strength of the solutions is increased to 0.1–0.2 M NaCl, the polyelectrolyte effects are largely suppressed, as indicated by the linear viscometric dependences (Equations 1 and 2). The data system shifts to the region of flexible chain macromolecules (points 3 and 6). Here, in MVAA-*co*-$MVAC_{12}H_{25}$ chains, hydrophobic interactions begin to manifest to a greater extent than in linear PSSNa chains. As the ionic strength increases the MVAA-*co*-$MVAC_{12}H_{25}$ [η] value decreases insignificantly (points 7, 8,

Figure 9). With a further increase in the ionic strength of solutions, MVAA-*co*-MVAC$_{12}$H$_{25}$ samples cease to dissolve molecularly. The mobility of -C$_{12}$H$_{25}$ side groups and their interaction in aqueous solutions are facilitated in comparison with the interactions of the elements of the same linear chain, as occurs in PSSNa chains. This is due to the fact that the side chains of graft copolymer chains are richer in entropy than linear chains of PSSNa. It is the copolymer side chains that cause hydrophobic interactions in these copolymers. Therefore, the manifestation of nonmolecular solutions and the onset of gelation occur earlier for MVAA-*co*-MVAC$_{12}$H$_{25}$ copolymers than for PSSNa.

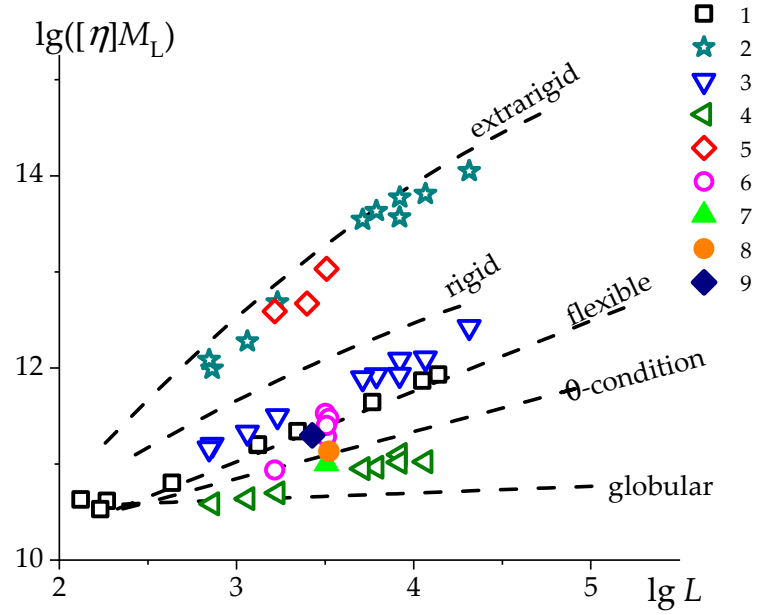

Figure 9. Normalized Kuhn-Mark-Houwink-Sakurada dependencies, (i.e., dependences of $[\eta]M_L$ characterizing the volume occupied by a chain segment corresponding to unit contour length of the macromolecule on the contour length of the macromolecule (M/M_L) in a double-logarithmic scale) for PMVA (M_L = 393 g/mol nm) [57] in H_2O (1); PSSNa (M_L = 750 g/mol nm) [54,59] in different aqueous compositions: H_2O (2), 0.2 M NaCl (3), 4.17 M NaCl (4); MVAA-*co*-MVAC$_{12}$H$_{25}$ (M_L = 468 g/mol nm) [55] in H_2O (5), in aqueous 0.1 M NaCl (6), 1 M NaCl (7), and 1.6 M NaCl (8) solutions; MVAA-*co*-MVAC$_{10}$H$_{21}$ (M_L = 452 g/mol nm) in aqueous 2 M NaCl solution (9). Dashed lines correspond to different conformations of linear chains: extra-rigid, rigid, flexible, globular, and θ-conditions [72,73].

Under the θ-condition (4.17 M NaCl, 25 °C), the PSSNa chains are additionally compressed (points 4) and their sizes fall between the θ-conditions for conventional flexible-chain polymers and the globular state. Under these conditions, the standard relation for PSSNa chains has the form: $[\eta]_{4.17\ M} = 0.0464M^{0.43\pm0.04}$, where the scaling index $b_\eta < 0.5$ that is, it becomes less than the minimum value allowed for linear macromolecules. Thus, the macromolecules of the strong polyelectrolyte PSSNa, going from top to the bottom, change their conformation from a slightly bent rod to a coil, and then approach the globular conformation, practically realizing the entire conformational spectrum of linear chain macromolecules.

4. Conclusions

The study of the viscous flow of dilute solutions of associating polymers allows to detect the presence of hydrophobic interactions in solutions already in the range of their sufficient dilution at $c[\eta] < 0.5$. Obtaining such information will require the comparative use of both the Huggins plot (η_{sp}/c on c) and the Kraemer plot ($\ln \eta_r/c$ on c), in a method we call the twin plot. It should be noted that this technique was quite well known in the early 50 s of the 20th century, but then forgotten. Indeed, new is well-forgotten old!

When interpreting the results of studying the viscous flow of polymer solutions, it should be taken into account that both $\lim_{c\to 0}(\eta_{sp}/c)$ and $\lim_{c\to 0}(\ln\eta_r/c)$ should converge at the same point. In this case, the concentration intervals used for linear extrapolation of the η_{sp}/c and $\ln\eta_r/c$ to $c \to 0$ can/should be different. Since always $|k''| < k'$, the interval used for extrapolation of η_{sp}/c to $c \to 0$ can be much shorter than that for $\ln\eta_r/c$ dependence. Recall that the *only* results/part of the results are obtained in the region of dilute polymer solutions when $c[\eta] < 1$ and $\eta_r < 2$, are the subject to analysis. The final measurement results must contain a single intrinsic viscosity value and correctly determined Kraemer and, especially, Huggins parameters. The values of the Huggins parameter exceeding 1, given anywhere in the literature, are overestimated. In turn, this leads to some underestimated $[\eta]$ values.

The parameter k'' is a sign-changing parameter, changing its sign from negative to positive for polymer systems exhibiting significant polymer–polymer interactions in solutions. Such systems include polymers in θ-solvents and amphiphilic copolymers of various topologies. Thus, the parameter k'' is a source of additional information about the manifestation of polymer–polymer interactions in solutions of macromolecular compounds.

The plot $\ln\eta_r$ vs. $c[\eta]$ is very informative when comparing homologous series of different kind of polymers or the same series in different solution conditions. This plot allows the series under study to be separated into hydrophilic or hydrophobic systems, depending on the sign of the curvature of the second-degree polynomial describing evolution of $\ln\eta_r$ in function of the degree of dilution. A positive sign corresponds to hydrophobic systems, and a negative one—to hydrophilic ones. A similar separation will occur between polymers in thermodynamically good solvents and polymer systems near θ-conditions.

A special situation arose in the study of amphiphilic polyelectrolytes in salt-free solutions. The results of the viscous flow of such solutions demonstrated the breach of homology, which also sometimes manifested under suppressed polyelectrolyte effects (compare sodium polystyrene-4-sulfonate and alkylated statistical copolymer N-methyl-N-vinyl acetamide and N-methyl-N-vinyl amine, Figures 5 and 6). Apparently, this can be associated with the irregular re-condensation of some of the counterions on the charged chain, which will lead to a random distribution of the charges remaining on the chain. This means a loss of homology and appears in the irregularity of $\ln\eta_r$ vs. $c[\eta]$ dependence. An informative and powerful tool in interpreting the molecular dependence of intrinsic viscosity is the use of the Kuhn-Mark-Houwink-Sakurada plot normalized to the mass per unit length of a linear polymer chain. Using the pattern established on the basis of the analysis of the literature data bank, one can semi-quantitatively establish the belonging of the studied polymer chains to one or another class of polymers. These possibilities were demonstrated on two series of polymers studied in various solvents.

Author Contributions: Conceptualization, G.M.P.; methodology, G.M.P.; validation, A.G., A.S.G. and O.D.; formal analysis, A.G., A.S.G., O.D. and O.O.; investigation, A.G., A.S.G., O.O. and O.D.; data curation, G.M.P.; writing—original draft preparation, A.G., O.D. and O.O.; writing—review and editing, G.M.P.; visualization, A.G., A.S.G. and O.D.; supervision, G.M.P.; project administration, G.M.P. All authors have read and agreed to the published version of the manuscript.

Funding: This research received no external funding.

Institutional Review Board Statement: Not applicable.

Data Availability Statement: Data is contained within the article.

Acknowledgments: The authors would like to thank the Corresponding Member of the Russian Academy of Sciences Evgenii Panarin and scientific researcher Irina Gavrilova for provided materials.

Conflicts of Interest: The authors declare no conflict of interest.

References

1. Winnik, M.A.; Yekta, A. Associative polymers in aqueous solution. *Curr. Opin. Colloid Interface Sci.* **1997**, *2*, 424–436. [CrossRef]
2. Hamley, I.W. *Block Copolymers in Solution: Fundamentals and Applications*; John Wiley & Sons: Hoboken, NJ, USA, 2005.
3. Liu, K.; Kang, Y.; Wang, Z.; Zhang, X. 25th Anniversary Article: Reversible and Adaptive Functional Supramolecular Materials: "Noncovalent Interaction" Matters. *Adv. Mater.* **2013**, *25*, 5530–5548. [CrossRef]
4. Krieg, E.; Bastings, M.M.; Besenius, P.; Rybtchinski, B. Supramolecular polymers in aqueous media. *Chem. Rev.* **2016**, *116*, 2414–2477. [CrossRef]
5. van der Tol, J.J.B.; Vantomme, G.; Palmans, A.R.A.; Meijer, E.W. Controlling the Processability and Stability of Supramolecular Polymers Using the Interplay of Intra- and Intermolecular Interactions. *Macromolecules* **2022**, *55*, 6820–6829. [CrossRef]
6. Kabanov, A.V.; Bronich, T.K.; Kabanov, V.A.; Yu, K.; Eisenberg, A. Soluble stoichiometric complexes from poly (N-ethyl-4-vinylpyridinium) cations and poly (ethylene oxide)-block-polymethacrylate anions. *Macromolecules* **1996**, *29*, 6797–6802. [CrossRef]
7. Burova, T.V.; Grinberg, N.V.; Grinberg, V.Y.; Tang, Y.; Zhang, G.; Khokhlov, A.R. Order-Disorder Conformational Transitions of N-Isopropylacrylamide−Sodium Styrene Sulfonate Copolymers in Aqueous Solutions. *Macromolecules* **2008**, *41*, 5981–5984. [CrossRef]
8. Nicolas, M.; Beyou, E.; Fumagalli, M. Two-step synthesis of polystyrene sulfonate based copolymers bearing pendant primary amines. *Eur. Polym. J.* **2021**, *152*, 110455. [CrossRef]
9. Piogé, S.; Fontaine, L.; Gaillard, C.; Nicol, E.; Pascual, S. Self-Assembling Properties of Well-Defined Poly(ethylene oxide)-b-poly(ethyl acrylate) Diblock Copolymers. *Macromolecules* **2009**, *42*, 4262–4272. [CrossRef]
10. Kawata, T.; Hashidzume, A.; Sato, T. Micellar structure of amphiphilic statistical copolymers bearing dodecyl hydrophobes in aqueous media. *Macromolecules* **2007**, *40*, 1174–1180. [CrossRef]
11. Shashkina, Y.A.; Zaroslov, Y.D.; Smirnov, V.A.; Philippova, O.E.; Khokhlov, A.R.; Pryakhina, T.A.; Churochkina, N.A. Hydrophobic aggregation in aqueous solutions of hydrophobically modified polyacrylamide in the vicinity of overlap concentration. *Polymer* **2003**, *44*, 2289–2293. [CrossRef]
12. Krayukhina, M.A.; Samoilova, N.A.; Yamskov, I.A. Polyelectrolyte complexes of chitosan: Formation, properties and applications. *Russ. Chem. Rev.* **2008**, *77*, 799. [CrossRef]
13. Ortona, O.; D'Errico, G.; Mangiapia, G.; Ciccarelli, D. The aggregative behavior of hydrophobically modified chitosans with high substitution degree in aqueous solution. *Carbohydr. Polym.* **2008**, *74*, 16–22. [CrossRef]
14. Lopez, C.G.; Colby, R.H.; Cabral, J.T. Electrostatic and Hydrophobic Interactions in NaCMC Aqueous Solutions: Effect of Degree of Substitution. *Macromolecules* **2018**, *51*, 3165–3175. [CrossRef]
15. Lu, A.; Wang, J.; Najarro, M.C.; Li, S.; Deratani, A. Synthesis and self-assembly of AB2-type amphiphilic copolymers from biobased hydroxypropyl methyl cellulose and poly (L-lactide). *Carbohydr. Polym.* **2019**, *211*, 133–140. [CrossRef] [PubMed]
16. Burova, T.V.; Grinberg, N.V.; Tur, D.R.; Papkov, V.S.; Dubovik, A.S.; Shibanova, E.D.; Bairamashvili, D.I.; Grinberg, V.Y.; Khokhlov, A.R. Ternary interpolyelectrolyte complexes insulin-poly (methylaminophosphazene)-dextran sulfate for oral delivery of insulin. *Langmuir* **2013**, *29*, 2273–2281. [CrossRef]
17. Adams, M.L.; Lavasanifar, A.; Kwon, G.S. Amphiphilic block copolymers for drug delivery. *J. Pharm. Sci.* **2003**, *92*, 1343–1355. [CrossRef]
18. Kedracki, D.; Abraham, J.N.; Prado, E.; Nardin, C. Self-Assembly of Biohybrid Polymers. In *Macromolecular Self-Assembly*; John Wiley & Sons: Hoboken, NJ, USA, 2016; pp. 193–229.
19. Moradi-Araghi, A. A review of thermally stable gels for fluid diversion in petroleum production. *J. Pet. Sci. Eng.* **2000**, *26*, 1–10. [CrossRef]
20. Abirov, R.; Ivakhnenko, A.P.; Abirov, Z.; Eremin, N.A. The associative polymer flooding: An experimental study. *J. Pet. Explor. Prod. Technol.* **2020**, *10*, 447–454. [CrossRef]
21. Gogoi, S.; Gogoi, S.B. Review on microfluidic studies for EOR application. *J. Pet. Explor. Prod. Technol.* **2019**, *9*, 2263–2277. [CrossRef]
22. Green, M.S.; Tobolsky, A.V. A New Approach to the Theory of Relaxing Polymeric Media. *J. Chem. Phys.* **1946**, *14*, 80–92. [CrossRef]
23. Rubinstein, M.; Dobrynin, A.V. Associations leading to formation of reversible networks and gels. *Curr. Opin. Colloid Interface Sci.* **1999**, *4*, 83–87. [CrossRef]
24. Rubinstein, M.; Dobrynin, A.V. Solutions of associative polymers. *Trends Polym. Sci.* **1997**, *5*, 181–186.
25. Semenov, A.N.; Rubinstein, M. Thermoreversible Gelation in Solutions of Associative Polymers. 1. Statics. *Macromolecules* **1998**, *31*, 1373–1385. [CrossRef]
26. Rubinstein, M.; Semenov, A.N. Thermoreversible gelation in solutions of associating polymers. 2. Linear dynamics. *Macromolecules* **1998**, *31*, 1386–1397. [CrossRef]
27. Zhang, Z.; Chen, Q.; Colby, R.H. Dynamics of associative polymers. *Soft Matter* **2018**, *14*, 2961–2977. [CrossRef] [PubMed]
28. Kujawa, P.; Audibert-Hayet, A.; Selb, J.; Candau, F. Rheological properties of multisticker associative polyelectrolytes in semidilute aqueous solutions. *J. Polym. Sci. Part B Polym. Phys.* **2004**, *42*, 1640–1655. [CrossRef]
29. Kujawa, P.; Audibert-Hayet, A.; Selb, J.; Candau, F. Effect of Ionic Strength on the Rheological Properties of Multisticker Associative Polyelectrolytes. *Macromolecules* **2006**, *39*, 384–392. [CrossRef]

30. Zhang, Z.; Huang, C.; Weiss, R.A.; Chen, Q. Association energy in strongly associative polymers. *J. Rheol.* **2017**, *61*, 1199–1207. [CrossRef]
31. Jiang, N.; Zhang, H.; Tang, P.; Yang, Y. Linear Viscoelasticity of Associative Polymers: Sticky Rouse Model and the Role of Bridges. *Macromolecules* **2020**, *53*, 3438–3451. [CrossRef]
32. Chassenieux, C.; Nicolai, T.; Benyahia, L. Rheology of associative polymer solutions. *Curr. Opin. Colloid Interface Sci.* **2011**, *16*, 18–26. [CrossRef]
33. Middleton, L.R.; Winey, K.I. Nanoscale aggregation in acid-and ion-containing polymers. *Annu. Rev. Chem. Biomol. Eng.* **2017**, *8*, 499–523. [CrossRef] [PubMed]
34. Staudinger, H.; Heuer, W. Über hochpolymere Verbindungen, 33. Mitteilung: Beziehungen zwischen Viscosität und Molekulargewicht bei Poly-styrolen. *Ber. Dtsch. Chem. Ges. A B Ser.* **1930**, *63*, 222–234. [CrossRef]
35. Wolff, C.; Silberberg, A.; Priel, Z.; Layec-Raphalen, M. Influence of the association of macromolecules in dilute solution on their reduced viscosity. *Polymer* **1979**, *20*, 281–287. [CrossRef]
36. Abdala, A.A.; Olesen, K.; Khan, S.A. Solution rheology of hydrophobically modified associative polymers: Solvent quality and hydrophobic interactions. *J. Rheol.* **2003**, *47*, 497–511. [CrossRef]
37. Pathak, J.A.; Nugent, S.; Bender, M.F.; Roberts, C.J.; Curtis, R.J.; Douglas, J.F. Comparison of Huggins Coefficients and Osmotic Second Virial Coefficients of Buffered Solutions of Monoclonal Antibodies. *Polymers* **2021**, *13*, 601. [CrossRef]
38. Roche, A.; Gentiluomo, L.; Sibanda, N.; Roessner, D.; Friess, W.; Trainoff, S.P.; Curtis, R. Towards an improved prediction of concentrated antibody solution viscosity using the Huggins coefficient. *J. Colloid Interface Sci.* **2022**, *607*, 1813–1824. [CrossRef]
39. Flory, P.J.; Fox, T.G. Treatment of Intrinsic Viscosities. *J. Am. Chem. Soc.* **1951**, *73*, 1904–1908. [CrossRef]
40. Kraemer, E.O. Molecular Weights of Celluloses and Cellulose Derivates. *Ind. Eng. Chem.* **1938**, *30*, 1200–1203. [CrossRef]
41. Rutgers, I.R. Relative viscosity and concentration. *Rheol. Acta* **1962**, *2*, 305–348. [CrossRef]
42. Budtov, V.P. *Physical Chemistry of Polymer Solutions*; Khimiya: Saint Petersburg, Russia, 1992; p. 381.
43. Lu, Y.; An, L.; Wang, Z.-G. Intrinsic Viscosity of Polymers: General Theory Based on a Partially Permeable Sphere Model. *Macromolecules* **2013**, *46*, 5731–5740. [CrossRef]
44. Lu, Y.; Shi, T.; An, L.; Jin, L.; Wang, Z.-G. A simple model for the anomalous intrinsic viscosity of dendrimers. *Soft Matter* **2010**, *6*, 2619–2622. [CrossRef]
45. Yan, D. Intrinsic viscosity of polymer solutions: Fresh ideas to an old problem. *Sci. China Chem.* **2015**, *58*, 835–838. [CrossRef]
46. Mead, D.J.; Fuoss, R.M. Viscosities of Solutions of Polyvinyl Chloride. *J. Am. Chem. Soc.* **1942**, *64*, 277–282. [CrossRef]
47. Huggins, M.L. The viscosity of dilute solutions of long-chain molecules. IV. Dependence on concentration. *J. Am. Chem. Soc.* **1942**, *64*, 2716–2718. [CrossRef]
48. Tsvetkov, V.N.; Eskin, V.E.; Frenkel, S.Y. *Structure of Macromolecules in Solution*; The National Lending Library for Science and Technology: London, UK, 1971.
49. Pamies, R.; Hernández Cifre, J.G.; del Carmen López Martínez, M.; García de la Torre, J. Determination of intrinsic viscosities of macromolecules and nanoparticles. Comparison of single-point and dilution procedures. *Colloid Polym. Sci.* **2008**, *286*, 1223–1231. [CrossRef]
50. Schoff, C. Concentration Dependence of the Viscosity of Dilute Polymer Solutions: Huggins and Schulz-Blaschke Constants. In *The Wiley Database of Polymer Properties*; John Wiley & Sons: Hoboken, NJ, USA, 2003.
51. Cohen, J.; Priel, Z.; Rabin, Y. Viscosity of dilute polyelectrolyte solutions. *J. Chem. Phys.* **1988**, *88*, 7111–7116. [CrossRef]
52. Weissberg, S.; Simha, R.; Rothman, S. Viscosity of dilute and moderately concentrated polymer solutions. *J. Res. Natl. Bur. Stand.* **1951**, *47*, 298–314. [CrossRef]
53. Gavrilova, I.I.; Panarin, E.F.; Nesterova, N.A. Homopolymerization of N-vinylamides in the presence of water-soluble initiators and preparation of polyelectrolytes from the polymerization products. *Russ. J. Appl. Chem.* **2012**, *85*, 413–416. [CrossRef]
54. Pavlov, G.M.; Okatova, O.V.; Gubarev, A.S.; Gavrilova, I.I.; Panarin, E.F. Strong Linear Polyelectrolytes in Solutions of Extreme Concentrations of One–One Valent Salt. Hydrodynamic Study. *Macromolecules* **2014**, *47*, 2748–2758. [CrossRef]
55. Pavlov, G.M.; Gosteva, A.A.; Okatova, O.V.; Dommes, O.A.; Gavrilova, I.I.; Panarin, E.F. Detection and evaluation of polymer–polymer interactions in dilute solutions of associating polymers. *Polym. Chem.* **2021**, *12*, 2325–2334. [CrossRef]
56. Pavlov, G.M.; Zaitseva, I.I.; Gubarev, A.S.; Gavrilova, I.I.; Panarin, E.F. Diffusion-viscometric analysis and conformational characteristics of sodium polystyrenesulfonate molecules. *Russ. J. Appl. Chem.* **2006**, *79*, 1490–1493. [CrossRef]
57. Pavlov, G.M.; Okatova, O.V.; Mikhailova, A.V.; Ulyanova, N.N.; Gavrilova, I.I.; Panarin, E.F. Conformational Parameters of Poly(N-methyl-N-vinylacetamide) Molecules Through the Hydrodynamic Characteristics Studies. *Macromol. Biosci.* **2010**, *10*, 790–797. [CrossRef] [PubMed]
58. Pavlov, G.; Zaitseva, I.I.; Mikhailova, N.A. Hydrodynamic and molecular characteristics of hydroxypropylmethyl cellulose and rheology of its aqueous solutions. *Polym. Sci. Ser. A* **2004**, *46*, 1068–1071.
59. Pavlov, G.M.; Gubarev, A.S.; Gavrilova, I.I.; Panarin, E.F. Conformations of sodium poly(styrene-4-sulfonate) macromolecules in solutions with different ionic strengths. *Polym. Sci. Ser. A* **2011**, *53*, 1003–1011. [CrossRef]
60. Pavlov, G.M.; Kolbina, G.F.; Okatova, O.V.; Gavrilova, I.I.; Panarin, E.F. Unimolecular micelles based on amphiphilic of N-methyl-N-vinylacetamide copolymers. *Dokl. Chem.* **2015**, *463*, 181–184. [CrossRef]
61. Dommes, O.A.; Gosteva, A.A.; Okatova, O.V.; Pavlov, G.M. Sizes Monitoring of Polyelectrolyte Flexible Chains over the Entire Range of Ionic Strength through Viscometry of Dilute Solutions. *Rev. Adv. Chem.* **2021**, *11*, 134–144. [CrossRef]

62. Lavrenko, P.N.; Okatova, O.V. New cell and methods of forming boundaries when studying macromolecular diffusion in solutions. *Polym. Sci. USSR* **1977**, *19*, 3049–3054. [CrossRef]
63. Tsvetkov, V.N. *Rigid-Chain Polymers: Hydrodynamic and Optical Properties in Solution*; Springer: New York, NY, USA, 1989; p. 490.
64. Schuck, P. Size-Distribution Analysis of Macromolecules by Sedimentation Velocity Ultracentrifugation and Lamm Equation Modeling. *Biophys. J.* **2000**, *78*, 1606–1619. [CrossRef]
65. Brown, P.H.; Schuck, P. A new adaptive grid-size algorithm for the simulation of sedimentation velocity profiles in analytical ultracentrifugation. *Comput. Phys. Commun.* **2008**, *178*, 105–120. [CrossRef]
66. Flory, P.J. *Principles of Polymer Chemistry*; Cornell University Press: Ithaca, NY, USA, 1953.
67. López Martínez, M.C.; Díaz Baños, F.G.; Ortega Retuerta, A.; García de la Torre, J. Multiple Linear Least-Squares Fits with a Common Intercept: Determination of the Intrinsic Viscosity of Macromolecules in Solution. *J. Chem. Educ.* **2003**, *80*, 1036. [CrossRef]
68. Gubarev, A.S. *Conformations of Water-Soluble Aromatic Macromolecules in Solutions of Various Ionic Strengths and Orientational Order in Films Prepared on Their Basis*; Saint Petersburg State University: Saint Petersburg, Russia, 2010.
69. Takahashi, A.; Kato, T.; Nagasawa, M. The Second Virial Coefficient of Polyelectrolytes. *J. Phys. Chem.* **1967**, *71*, 2001–2010. [CrossRef]
70. Pavlov, G.M.; Gubarev, A.S. Intrinsic viscosity of strong linear polyelectrolytes in solutions of low ionic strength and its interpretation. In *Advances in Physicochemical Properties of Biopolymers: Part 1*; Bentham Science Publishers BV: Sharjah, United Arab Emirates, 2017; pp. 433–460.
71. Kurata, M.; Tsunashima, Y. Viscosity—Molecular Weight Relationships and Unperturbed Dimensions of Linear Chain Molecules. In *The Wiley Database of Polymer Properties*; John Wiley & Sons: Hoboken, NJ, USA, 2003.
72. Pavlov, G.; Harding, S.; Rowe, A. Normalized scaling relations as a natural classification of linear macromolecules according to size. In *Analytical Ultracentrifugation V*; Springer: Berlin/Heidelberg, Germany, 1999; pp. 76–80.
73. Pavlov, G.M. Size and average density spectra of macromolecules obtained from hydrodynamic data. *Eur. Phys. J. E* **2007**, *22*, 171–180. [CrossRef] [PubMed]
74. Pavlov, G.M. Hydrodynamics of Macromolecules: Conformation Zoning for General Macromolecules. In *Encyclopedia of Biophysics*; Roberts, G., Watts, A., Eds.; Springer: Berlin/Heidelberg, Germany, 2020; pp. 1–13.
75. Pavlov, G.M.; Dommes, O.A.; Okatova, O.V.; Gavrilova, I.I.; Panarin, E.F. Spectrum of hydrodynamic volumes and sizes of macromolecules of linear polyelectrolytes versus their charge density in salt-free aqueous solutions. *Phys. Chem. Chem. Phys.* **2018**, *20*, 9975–9983. [CrossRef] [PubMed]